

Replication of nanopits and nanopillars by roll-to-roll extrusion coating using a structured cooling roll

Murthy, Swathi; Pranov, Henrik; Pedersen, Henrik Chresten; Taboryski, Rafael J.

Published in:

Journal of Vacuum Science and Technology. Part B. Nanotechnology & Microelectronics

Link to article, DOI:

[10.1116/1.4967217](https://doi.org/10.1116/1.4967217)

Publication date:

2016

Document Version

Publisher's PDF, also known as Version of record

[Link back to DTU Orbit](#)

Citation (APA):

Murthy, S., Pranov, H., Pedersen, H. C., & Taboryski, R. J. (2016). Replication of nanopits and nanopillars by roll-to-roll extrusion coating using a structured cooling roll. *Journal of Vacuum Science and Technology. Part B. Nanotechnology & Microelectronics*, 34(6), [06KM02]. DOI: 10.1116/1.4967217

DTU Library

Technical Information Center of Denmark

General rights

Copyright and moral rights for the publications made accessible in the public portal are retained by the authors and/or other copyright owners and it is a condition of accessing publications that users recognise and abide by the legal requirements associated with these rights.

- Users may download and print one copy of any publication from the public portal for the purpose of private study or research.
- You may not further distribute the material or use it for any profit-making activity or commercial gain
- You may freely distribute the URL identifying the publication in the public portal

If you believe that this document breaches copyright please contact us providing details, and we will remove access to the work immediately and investigate your claim.

Replication of nanopits and nanopillars by roll-to-roll extrusion coating using a structured cooling roll

Swathi Murthy, Henrik Pranov, Henrik C. Pedersen, and Rafael Taboryski

Citation: *Journal of Vacuum Science & Technology B* **34**, 06KM02 (2016); doi: 10.1116/1.4967217

View online: <http://dx.doi.org/10.1116/1.4967217>

View Table of Contents: <http://scitation.aip.org/content/avs/journal/jvstb/34/6?ver=pdfcov>

Published by the AVS: Science & Technology of Materials, Interfaces, and Processing

Articles you may be interested in

[Roll-to-roll UV imprinting lithography for micro/nanostructures](#)

J. Vac. Sci. Technol. B **33**, 060801 (2015); 10.1116/1.4933347

[Fabrication of antireflection structure film by roll-to-roll ultraviolet nanoimprint lithography](#)

J. Vac. Sci. Technol. B **32**, 06FG09 (2014); 10.1116/1.4901877

[High-density pattern transfer via roll-to-roll ultraviolet nanoimprint lithography using replica mold](#)


J. Vac. Sci. Technol. B **30**, 06FB07 (2012); 10.1116/1.4758922





[High aspect ratio fine pattern transfer using a novel mold by nanoimprint lithography](#)

J. Vac. Sci. Technol. B **29**, 06FC15 (2011); 10.1116/1.3662080

[Overcoming material challenges for replication of “motheye lenses” using step and flash imprint lithography for optoelectronic applications](#)

J. Vac. Sci. Technol. B **26**, 1794 (2008); 10.1116/1.2981081


Instruments for Advanced Science

<p>Contact Hiden Analytical for further details: W www.HidenAnalytical.com E info@hiden.co.uk</p> <p>CLICK TO VIEW our product catalogue</p>	 <p>Gas Analysis</p> <ul style="list-style-type: none"> › dynamic measurement of reaction gas streams › catalysis and thermal analysis › molecular beam studies › dissolved species probes › fermentation, environmental and ecological studies 	 <p>Surface Science</p> <ul style="list-style-type: none"> › UHV TPD › SIMS › end point detection in ion beam etch › elemental imaging - surface mapping 	 <p>Plasma Diagnostics</p> <ul style="list-style-type: none"> › plasma source characterization › etch and deposition process reaction › kinetic studies › analysis of neutral and radical species 	 <p>Vacuum Analysis</p> <ul style="list-style-type: none"> › partial pressure measurement and control of process gases › reactive sputter process control › vacuum diagnostics › vacuum coating process monitoring
--	--	--	--	--

Replication of nanopits and nanopillars by roll-to-roll extrusion coating using a structured cooling roll

Swathi Murthy^{a)}

Inmold A/S, Gregersensvej 6, DK-2630 Taastrup, Denmark and Department of Photonics Engineering, Technical University of Denmark, Frederiksborgvej 399, DK-4000 Roskilde, Denmark

Henrik Pranov

Inmold A/S, Gregersensvej 6, DK-2630, Taastrup, Denmark

Henrik C. Pedersen

Department of Photonics Engineering, Technical University of Denmark, Frederiksborgvej 399, DK-4000 Roskilde, Denmark

Rafael Taboryski^{b)}

Department of Micro- and Nanotechnology, Technical University of Denmark, Ørstedes Plads, Building 345b, DK-2800 Kongens Lyngby, Denmark

(Received 27 June 2016; accepted 24 October 2016; published 8 November 2016)

This paper investigates a novel, very high throughput, roll-to-roll (R2R) process for nanostructuring of polymer foils, called R2R extrusion coating. It has the potential to accelerate the integration of nanostructured materials in consumer products for a variety of applications, including optical, technical, and functional surfaces and devices. In roll-to-roll extrusion coating, a molten polymer film is extruded through a flat die forming a melt curtain, and then laminated onto a carrier foil. The lamination occurs as the melt curtain is pressed between a cooling roller and a counter roller. By mounting a nanostructured metal shim on the surface of the cooling roller, the relief structure from the shim can be replicated onto a thermoplastic foil. Among the benefits of P_{oil} , the process are availability of a wide range of commercial extruders, off-the-shelf extrusion grade polymers, functional additives, polymeric materials with good diffusion barrier properties, and the overall maturity of the technology [S. H. Ahn and L. J. Guo, *Adv. Mater.* **20**, 2044 (2008)]. In this article, the authors demonstrate replication of nanopits and nanopillars with diameters between 40 and 120 nm and depth/height of 100 nm. The best replication was achieved in polypropylene, by running at high roller line-speed of 60 m/min, and high cooling roller temperature of 70 °C. Replication in other common polymers like polyethylene and polystyrene was not possible for the parameter range used for the investigation. © 2016 Author(s). All article content, except where otherwise noted, is licensed under a Creative Commons Attribution (CC BY) license (<http://creativecommons.org/licenses/by/4.0/>). [<http://dx.doi.org/10.1116/1.4967217>]

I. INTRODUCTION

Micro and nanostructuring of material surfaces can provide new valuable functionalities like superhydrophobic surfaces,¹ antireflective surfaces,² and structural colors.³ Apart from a few exceptions [like compact discs (CDs), digital versatile disc (DVDs)], nanostructured polymer materials have not penetrated the consumer market mainly due to high manufacturing costs associated with the complexity and large number of processing steps involved to manufacture them.

Injection molding (IM) is a well-known industrial technology platform for mass production of polymer items used in our daily life, from water bottles to automotive components. Research and development is being conducted worldwide to adapt this technique to manufacture nanomicrostructured surfaces in thermoplastic polymers. However, there is a limit to the minimum feature size that can be replicated by traditional IM setup, due to rapid cooling of the molten polymer when it comes in contact with the metallic mold surface. The polymer

solidifies before completely filling the nano-micro-structures on the mold. Many research groups and industries have attempted to adapt specialized IM setups to overcome this issue. One of them is injection compression molding, used in the manufacturing of CDs and DVDs. This can replicate sub-micrometer features. However, high aspect ratio structures cannot be replicated by this method. The maximum aspect ratio reported for this method is ~ 2 .⁴ Another specialized IM set-up is variothermal injection molding, used to replicate high aspect ratio structures and small feature sizes with high fidelity. The drawback of this method is that it needs elaborate mechanisms and incorporation of complex systems into the tool.^{5,6} It also suffers from relatively high cycle times and hence low production rates. Recently, a research group has demonstrated replication of high aspect ratio structures, >10 , by adapting heat retardation technique, using polymer injection molds.⁷ Few of the other recent progresses in injection molding have been fabrication of super hydrophobic polymer parts.^{8,9} Though polymer nanostructures down to 25 nm can be replicated and a wide range of polymers can be molded by specialized IM,¹⁰ it is only capable of producing parts with substantial rigidity.

^{a)}Electronic mail: sm@inmold.dk

^{b)}Electronic mail: rata@nanotech.dtu.dk

To achieve high throughput fabrication of nanostructures surfaces on flexible substrate materials, roll-to-roll (R2R) technologies seem to be promising candidates.^{11–13} The molding and demolding processes run continuously in a R2R setup, thereby significantly increasing the throughput. It also has the advantage of better uniformity.¹² It requires less force during replication, since the contact area between the mold and the polymer is small, compared to large area planar molding. The release force is also much less due to the peeling action of the mold rotating away from the substrate. Thereby, R2R production causes relatively less damage to the mold and reduces defects in the structured polymer. The two existing R2R processes, R2R ultraviolet nanoimprint lithography (R2R UV-NIL) and R2R hot embossing (R2R-HE), each have drawbacks. In R2R UV-NIL, the pattern transfer is done by pressing a transparent structured roller into a UV-curable material layer, which upon UV-illumination is cross-linked. Though the replication fidelity is high, only few specialized materials are compatible with this process.¹¹ Another process, R2R-HE presses a mold (nanorelief plate) mounted on a roll into a thermoplastic foil, while heating it above its solidification temperature and thereby transferring the pattern.¹² This process suffers from wear issues of the mold, poor replication fidelity.¹⁴ Since the pattern replication depends on the contact time, this sets a limit on the roller speed; hence, it also has a relatively low-throughput.¹⁵

To overcome the above mentioned limitations of the existing mass production technologies for nano-micro-structuring of polymer surfaces, we investigate a true high throughput, and low cost production technique with high replication fidelity, called R2R extrusion coating (R2R-EC), for large scale nanopatterning into standard thermoplastic polymers. R2R-EC is a mature industrial production technology with inherently ultrahigh-throughput (5 m²/s and higher).¹⁶ The economic benefit of using R2R-EC lies in the availability of a wide range of R2R-EC machines. In addition, off-the-shelf extrusion grade polymers are available for most thermoplastic polymer families. Finally, the maturity of the technology has allowed for robust machinery and cost of polymer materials to reach a minimum. Relatively low pressure is required during replication in R2R-EC as compared to previously mentioned R2R technologies, allowing one to use longer cylindrical molds. This, combined with high roll speed, can give a very high throughput, >5 m²/s. The simplicity of the process allows for compatibility with many different thermoplastic polymer materials. R2R-EC is used today, mostly, to manufacture smooth plastic foil. Replication of nano- and microstructures by R2R-EC has been investigated for the first time in our previous work.^{17,18} In this paper, we aim to provide a deeper insight into the replication of nanopits and nanopillars by this method.

II. EXPERIMENT

A. Si master fabrication

Si masters of 2 in. were fabricated by electron beam lithography using JEOL 100 kV e-beam lithography tool followed by deep reactive ion etch. Structures of diameter (D) from 40

to 120 nm and pitch (P) from 80 to 240 nm were exposed onto an e-beam resist. A spin coated positive resist ZEP-520A (Zeon chemicals) was used for fabrication of pits in Si. A spin coated negative resist ARN-7520 (Allresist) was used for fabrication of pillars in Si. After pattern exposure and development, the structures were etched into the Si wafer, by a Pegasus deep reactive-ion etching system (SPTS Technologies, Ltd.), using the developed resist film as an etch mask. The remaining resist was removed by oxygen plasma. The Si masters were then used to fabricate ductile Ni shims by electroplating.

B. Ni mold fabrication

Ni molds of 2 in. were fabricated using a standard dry etching, electroplating, and molding process.^{19,20} First, a 15–25 nm thin seed layer of nickel-vanadium alloy (7 wt. % vanadium) was sputter coated (Polyteknik Cryofox Explorer 700) on structured Si master (explained in Sec. II C), followed by electroplating in a galvanic nickel bath (Technotrans microform.200) to form 175–200 μm thick nickel molds. To enable easy demolding of polymer replica during extrusion coating, Ni molds were coated with a perfluorodecyltrichlorosilane (FDTS) antistiction layer. First, a thin layer of Al₂O₃ was deposited on Ni shims, by atomic layer deposition (Picosun ALD model R200), before molecular vapor deposition of FDTS (Applied Microstructures, Inc., MVD 100), to enable good adhesion between Ni shims and FDTS. A summary of the process steps involved in the fabrication of Ni mold is presented in Fig. 1.

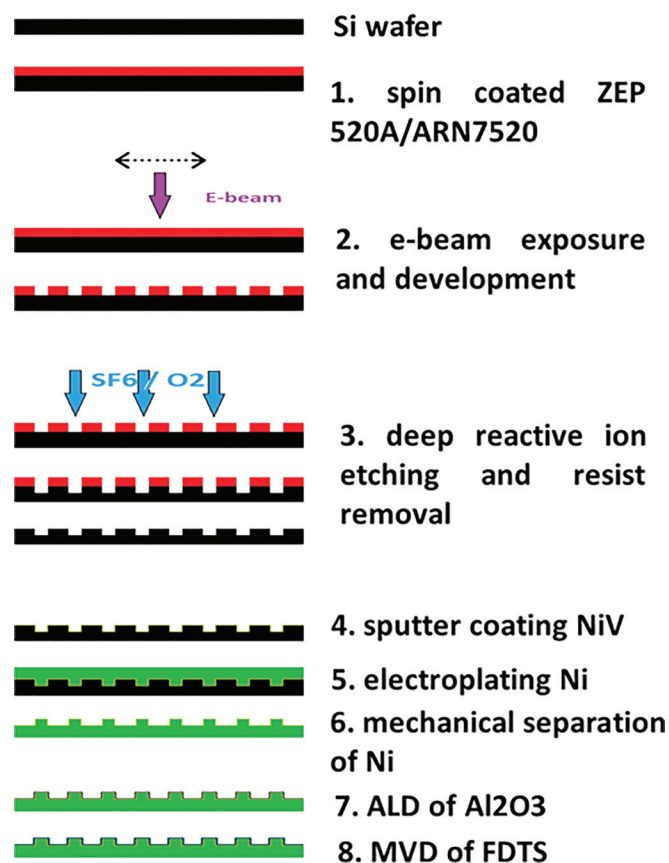


FIG. 1. (Color) Schematic diagram of Ni mold fabrication.

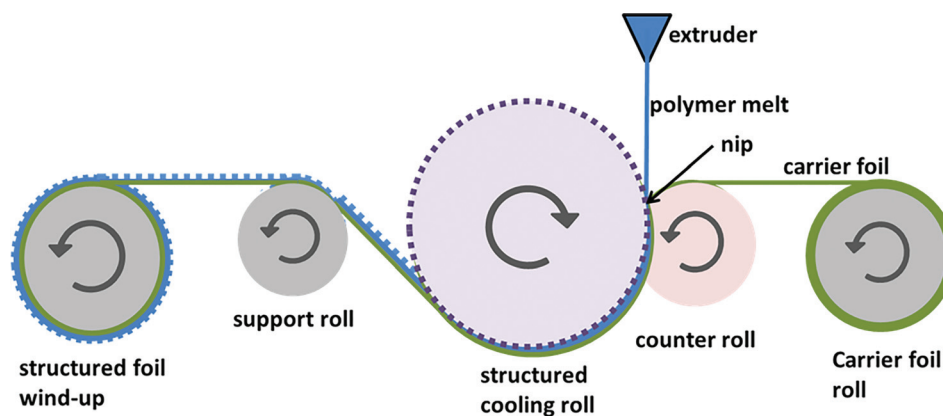


FIG. 2. (Color) Schematic of the R2R-EC process.

C. R2R-EC using structured cooling roll

The nanostructured foils presented in this paper were produced by extrusion coating on a pilot R2R-EC machine, at Danapak Flexibles A/S, Slagelse, Denmark. It consists of a 25 mm extruder (BfA Plastic GmbH), 35 mm extruder (AXON Plastics Machinery AB), and an EPOCH nozzle with a respective three-layer feedblock (Cloeren, Inc.).

During the R2R-EC, a ~ 5 mm thick film of molten polymer at a temperature of 300°C and a constant feed rate of 30 g/m^2 and width ~ 45 cm is extruded through a flat die and coated onto a polyethylene terephthalate (PET) carrier foil, in the contact area formed between the structured cooling roll and the flexible pressure (counter) roll, called the nip (as shown in Fig. 2). Two inches nanostructured Ni shims (explained in Sec. II B) were mounted onto the cooling roll using a double-sided adhesive tape. The width of the cooling roller is ~ 45 cm. The temperature of the cooling roll (T_C) was kept below the solidification temperature of the polymer by running water through it. The pressure roll consists of a metal core wrapped with a 10–15 mm thick layer of silicone rubber, making it flexible on the surface. The pressure roll is maintained at room temperature using cooling water. Force to the pressure roll (measured as oil pressure— P_{oil}) is provided by two hydraulic pistons attached at each end of the shaft. The area of the two hydraulic pistons is 31 cm^2 each. The rolls are not motorized, and the drive is provided by the substrate drawn by the winder (motorized winding roll), creating a line tension, resulting in a line speed (V_R), which can be controlled. The nip is the most critical part in the setup, where the replication of nanostructures takes place under pressure. After the nip, the polymer is wrapped around the cooling roll with the help of the support roll before being wound up onto another roll. No cooling phase is required as the polymer solidifies rapidly due to the large thermal mass of the mold, keeping the fabrication time low and a very high throughput. The final extruded films were quite uniform, with $<0.1\%$ variation in thickness across the web width (from center of the web to the edges) and the same thickness across the web length. The uniformity of the extruded foil was determined by cutting out several circular foil samples, of $D = 10$ cm, across the width and length of the web and weighing them precisely. Any difference in

weight between the samples would directly correspond to the thickness variation in the extruded polymer.

D. Polymers investigated for R2R-EC

We investigated various polymers, like pure polypropylene (PP)—WF420HMS, Borealis, low density polyethylene (LDPE)—3020D, LyondellBasell, and polystyrene (PS)—BASF PS 158 K, for replication of nanostructures. Different sets of processing parameters were investigated to assess their influence on the replication fidelity. Specifically, the influence of cooling roller temperature T_C (30 – 70°C), line speed V_R (10 – 60 m/min) and the hydraulic pressure P_{oil} (5 – 22 bars) were explored separately, while keeping all other parameters constant. For the parameteric analysis, extruder output, melt temperature, feed rate, die gap, and air gap height were kept constant.

E. Characterization of structured foils

For each set of process parameters in R2R-EC, several meters of polymer foil was produced. The replication was assessed and compared for samples across different parameter sets. The results shown in this paper are from either scanning electron microscopy [(SEM) Zeiss Supra VP 40 or VP 60 SEM] and/or atomic force microscopy [(AFM) Park Systems Corporation XE-150]. Prior to SEM, the polymer foils were sputter coated with a 8–10 nm thin film of gold-palladium (Au-Pd).

III. THERMOMECHANICAL ANALYSIS OF THE NIP

R2R-EC is a combination of polymer extrusion, stretching of the melt curtain in air before the calendaring step, to apply the film onto a carrier foil. The molten polymer is extruded through a flat die and coated on a PET carrier foil and then passed through the nip. In this study, the nip consists of a nanostructured cooling roll (cooled by water) and a pressure roll covered with silicone rubber. In the nip, the polymer film is pressed against the cooling roll and simultaneously cooled by it. The residence time of the polymer melt in the nip is in the order of few milliseconds, depending on V_R . A detailed simulation of the thermal and pressure profiles in the nip has been shown in our previous work.¹⁷ The

nip pressure (P_{nip}) along the nip is calculated using Hertz theory of dry contact given by the following equation:¹⁷

$$P_{\text{nip}} = P_{\text{max}} \sqrt{1 - \left(\frac{L_{\text{nip}} - 2x}{L_{\text{nip}}} \right)^2}, \quad (1)$$

$P_{\text{max}} = F/\pi WL_{\text{nip}}$, x is the distance along the nip from the starting point, L_{nip} is length of the nip and W is the width of the cooling roll, F = nip force = area of the two pistons times P_{oil} . The result indicates that P_{max} is at the center of the nip. As P_{oil} and hence the F is increased, the L_{nip} and the P_{max} across the nip also increases. L_{nip} was measured by passing a flexible tape through the nip under different P_{oil} and measuring the length of the footprint. For $P_{\text{oil}} = 22$ bars, L_{nip} was measured to be ~ 18 mm; for $P_{\text{oil}} = 5$ bar, L_{nip} was ~ 12 mm.

COMSOL simulation of the temperature profile in the nip for different V_R has been explained in detail in our previous work.¹⁷ The simulation results show that PP cools almost instantaneously near the mold surface (in the order of 10^6 °C/s) and relatively slowly in the bulk of the polymer melt away from the mold–melt interface, this is because of the high thermal conductivity of Ni compared to polymer (PP or PET). The simulation results indicate that V_R is an important factor affecting the temperature profile in the nip. At 100 nm from the mold surface, the polymer solidifies closer to the center of the nip for higher V_R than at lower V_R [Fig. 3(c)].

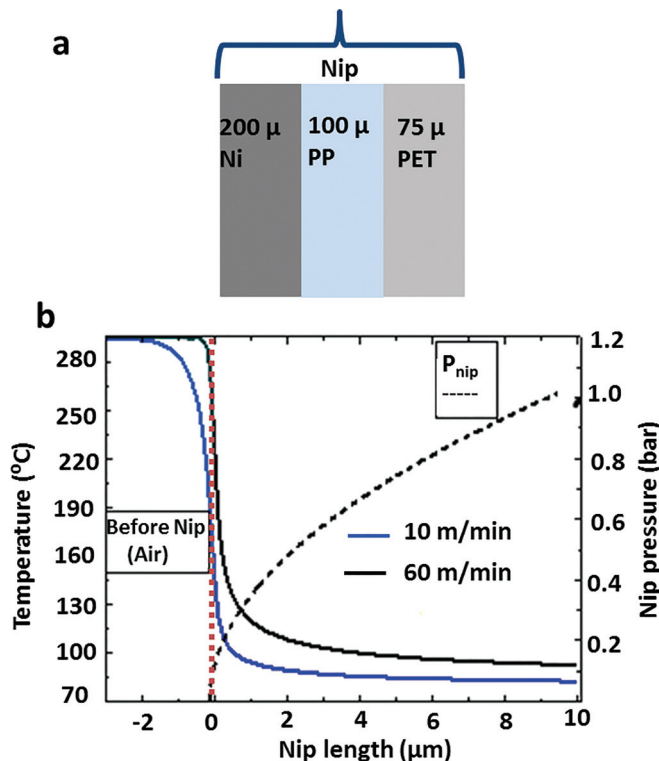


FIG. 3. (Color) (a) Schematic representation of the nip used for COMSOL simulation; (b) simulated temperature profile in the nip at 100 nm from the mold surface for $P_{\text{oil}} = 22$ bars and $V_R = 60$ and 10 m/min; calculated nip pressure (P_{nip}) across the nip length for $P_{\text{oil}} = 22$ bars using Hertz theory for dry contact.

This means that at higher V_R the polymer melt experiences higher contact pressure, before it solidifies, than at lower V_R , which can assist in better replication of nanostructures.

IV. RESULTS AND DISCUSSION

A. Influence of process parameters: P_{oil} , T_C , and V_R

Similar to injection molding and nanoimprint lithography, in extrusion coating, we observed a general trend of better replication quality with higher nip pressure (result of P_{oil}), higher T_C . The best replication of nanostructures was achieved for high $V_R = 60$ m/min, high $P_{\text{oil}} = 22$ bars, and high $T_C = 70$ °C.

1. Replication of nanopillars by R2R-EC

We have, so far, been able to replicate nanopillars down to $D = 40$ nm, $P = 120$ nm, and height = 100 nm by R2R-EC in PP (Fig. 4). The limiting factor to replicate smaller pillars has been Ni mold fabrication. The cracks visible in the SEM images (Figs. 4–7) are in the sputtered Au-Pd layer and not the extruded polymer foil. As the polymer samples are nonconductive, the Au-Pd layer is sputter coated to form a conductive surface, necessary for SEM to avoid charging effects.

The effect of T_C and V_R on the replication of nanopillars ($D \sim 100$ nm, $P \sim 200$ nm, and height ~ 100 nm) in PP, at P_{oil} of 22 bars, is shown in Fig. 5. We observed an improved replication at higher T_C and higher V_R . $V_R = 60$ m/min was the limit of the pilot extrusion coating machine used for the investigation and the mold temperature of 70 °C was limited by the adhesive tape used for mounting of the Ni mold on the roller, because the tape would melt at temperatures higher than 70 °C. At $P_{\text{oil}} = 22$ bars, the best replication (in terms of shape and height of the pillars as compared to the Si master) was achieved at $T_C = 70$ °C and $V_R = 60$ m/min, whereas at $T_C = 30$ °C and $V_R = 10$ m/min, the pillars were only 50% replicated in terms of height, indicating incomplete mold filling. As explained in Sec. III, the improved replication at higher line speed (keeping other parameters

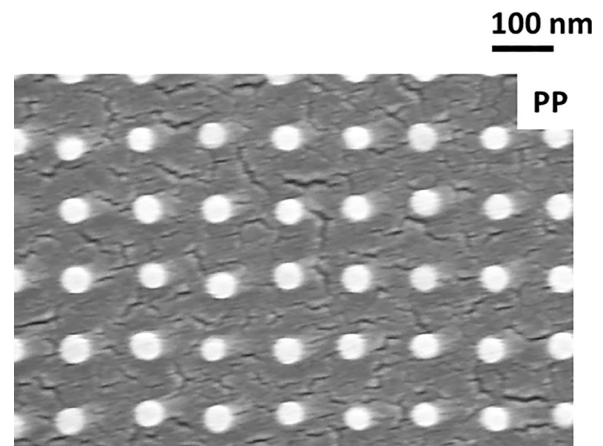


FIG. 4. SEM image of smallest pillars replicated in PP by -R2R-EC at $P_{\text{oil}} = 22$ bars, $T_C = 70$ °C, and $V_R = 60$ m/min. $D = 40$ nm, average height = 100 nm, and $P = 120$ nm. The visible cracks originate from the Au-Pd coating applied to ease the visualization by SEM.

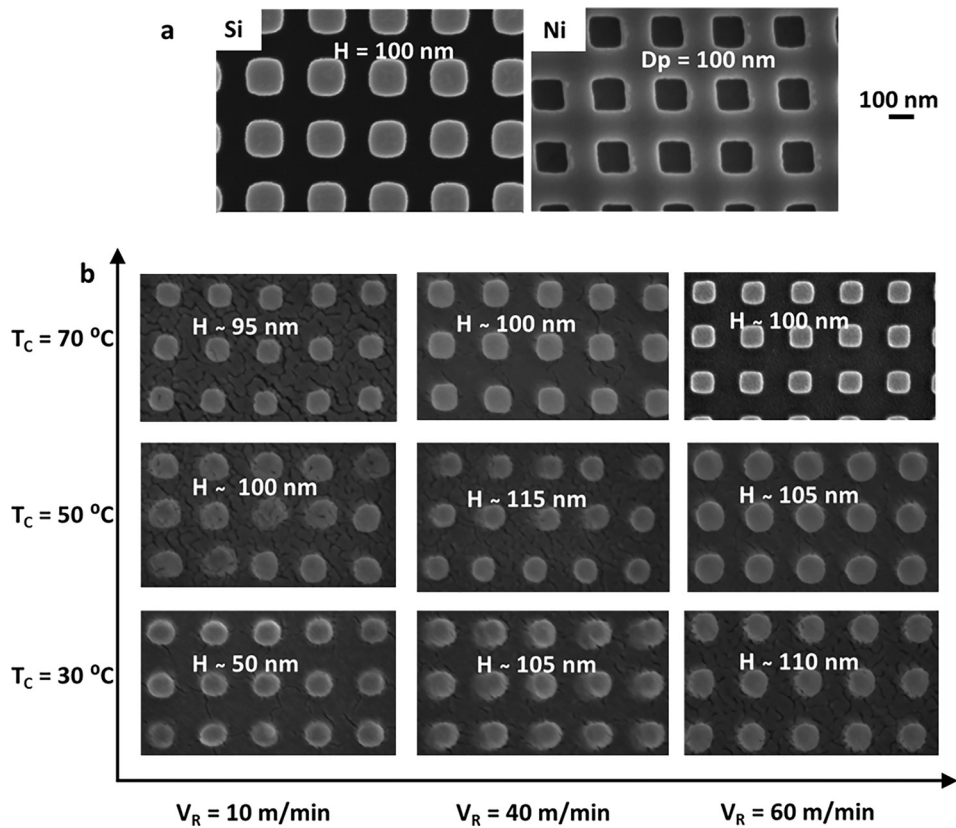


FIG. 5. (a) SEM images of Si master (H:average height of nanopillars) and Ni shim (Dp:average depth of nanoholes). (b) Nanopillar arrays replicated in PP at $P_{oil} = 22$ bars, different T_C and V_R ; H of the pillars in (b) was measured by AFM over an area of $4 \mu m^2$. Dimensions of the nanostructures: $D = 100$ nm and $P = 200$ nm.

constant) could be because the PP melt solidifies closer to the center of the nip for $V_R = 60$ m/min as compared to $V_R = 10$ m/min. This means PP experiences higher nip pressure at $V_R = 60$ m/min than at $V_R = 10$ m/min, resulting in better replication.

2. Replication of nanopits by R2R-EC

We have, so far, been able to replicate nanopits down to $D = 60$ nm, $P = 100$ nm, and depth = 100 nm by R2R-EC

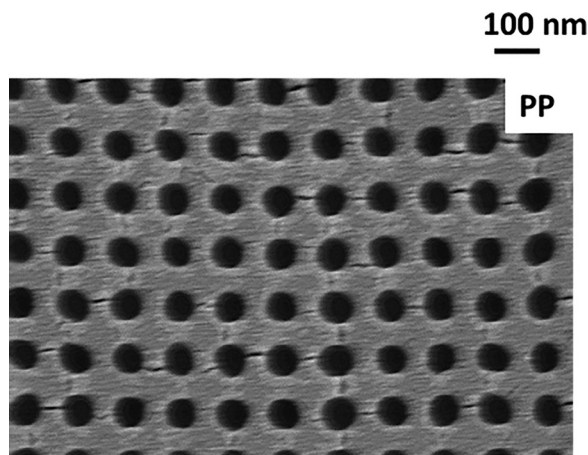


FIG. 6. SEM image of smallest pits replicated in PP by nano-R2R-EC at $P_{oil} = 22$ bars, $T_C = 70$ °C, and $V_R = 60$ m/min. $D = 60$ nm, average depth (measured by AFM) ~ 100 nm, and $P = 100$ nm.

(Fig. 6). The limiting factor to fabricate smaller structures has been Ni mold fabrication. We observed a similar parameter trend for replication of nanopits as for nanopillars (described in Sec. IV A 1, Fig. 5). The best achieved replication for nanopits in PP, for parameter range used, was also at $P_{oil} = 22$ bars, $T_C = 70$ °C, and $V_R = 60$ m/min (example in Fig. 7).

B. Influence of polymer material for replication in R2R-EC

For the parameter range used for the investigation, replication of nanostructures from Ni mold by R2R-EC was, so far, observed only in PP. There was no visible replication in LDPE, which is also a semicrystalline polymer and PS, which is an amorphous polymer. To understand these results, we adapted Laplace-young equation of capillarity which gives the relation between surface tension (γ), capillary pressure (ΔP), and principle radius of curvature R_L of fluid air interface

$$R_L = \frac{2\gamma}{\Delta P}. \quad (2)$$

In the present scenario, ΔP is P_{nip} , R_L the Laplace radius of curvature of the polymer melt droplet, whereas γ is the surface tension of the polymer melt at the corresponding point in the nip.

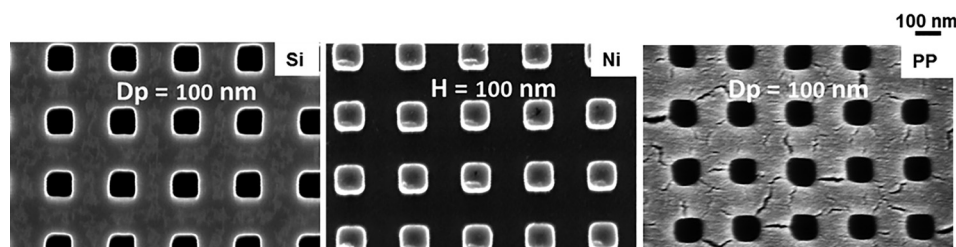


Fig. 7. SEM images of nanopits in Si master (D_p : average depth of nanoholes), corresponding nanopillars in Ni mold (H : average height of nanopillars) and nanoholes replicated in PP foil by extrusion coating at $P_{oil} = 22$ bars, $T_c = 70^\circ\text{C}$, and $V_R = 60$ m/min. Dimensions of nanostructures: $D = 100$ nm and $P = 200$ nm.

The following discussion is for $T_C = 70^\circ\text{C}$, $P_{oil} = 22$ bars, and $V_R = 60$ m/min. It is a well-known fact that surface tension of polymer melts influence the filling of the structures during microinjection molding.²¹ The effect of surface tension increases with the decrease in the feature size. It has been reported by previous studies that surface tension can reduce the melt filling time in microstructures.²¹ Yang *et al.* made experimental measurements of surface tension of different polymers using axisymmetric drop shape analysis method in N_2 environment.²² They found that surface tension for polymer melt decreases linearly with the increase in the polymer melt temperature (T_m). The following equation was obtained, for PP, PE, and PS, using linear fit of their experimental data:

$$\gamma(T) = \alpha - \beta T_m. \quad (3)$$

Here, $\gamma(T)$ is in mN/m. The constants α and β as reported by Yang *et al.*²² and T_m for different polymers are shown in Table I.

By following the temperature profile in Fig. 3(b) and obtaining the corresponding P_{nip} from Eq. (1) and substituting T_m for different polymers obtained from literature,^{23,24} R_L obtained for different polymers at T_m , from Eqs. (2) and (3) at their respective T_m is shown in Table I. Considering the nanopillars shown in Fig. 5, in order to completely fill the nanopits in the mold, including the corners, R_L should be smaller than the radius of the nanopits (R_h) in the mold, i.e., < 50 nm for nanopits in Fig. 5.

PS is an amorphous polymer and it solidifies at T_m and cannot be super-cooled. From Table I, R_L for PS is $\sim 1.2 \mu\text{m}$, which is much higher than R_h . Hence, we do not see any replication of the nanopillars in PS. PE is a semicrystalline polymer and can be super-cooled to a certain extent, and its crystallization rate is extremely high (compared to PP). This means that PE solidifies quickly below its T_m ($\sim 110^\circ\text{C}$).²⁵⁻²⁸ Hence, R_L for PE does not become small enough to fill the nanopits in the mold. This could be the reason we do not see any replication of nanopillars in PE as well.

TABLE I. Parameters for the different polymers used for the investigation.

Polymer	T_m ($^\circ\text{C}$)	α (mN/m)	β [mN/(m $^\circ\text{C}$)]	γ (T_m) (mN/m)	P_{nip} (T_m) (kPa)	R_L (T_m) (μm)	Crystallinity
PP	~ 180	27.734	0.059	17.11	22	~ 1.5	Semicrystalline
LDPE	~ 110	31.463	0.032	27.943	45	~ 1.2	Semicrystalline
PS	~ 100	39.305	0.070	32.302	63	~ 1.2	Amorphous

PP is also a semicrystalline polymer, like PE, and can be super-cooled for a considerable amount of time, as it has a relatively slow crystallization rate. From Fig. 3(b), the calculated cooling rate of polymer melt at 100 nm from the mold surface is $\sim 10^6$ $^\circ\text{C/s}$. We cannot measure the crystallization rate of PP at such high cooling rate with the currently available equipment and methods. The maximum cooling rates that can be presently attained by flash differential scanning calorimetry is only $\sim 10^4$ $^\circ\text{C/s}$.²⁹ The half crystallization time for PP at 80°C is reported in literature to vary between 0.2 and 10 s.^{29,30} Once the polymer melt enters the nip, it takes about 9 ms to reach the center of the nip (9 mm at 60 m/min), where the pressure is maximum and hence R_L is minimum. Since we observe complete replication of nanopillars in PP at 60 m/min, it indicates that solidification of PP is retarded by sufficient amount of time, such that it can attain a very small R_L , and flow into the nanopits in the mold. This also explains why the replication of nanopillars (Fig. 5) gets worse at lower V_R and lower T_C , as PP could have solidified completely before it can attain a small enough R_L .

C. Mold life time

SEM images of the Ni mold were taken before and after R2R-EC on the pilot extruder. As shown in Fig. 8, Ni mold with nanopits remains almost intact after R2R-EC of hundreds of meters of foil, whereas Ni mold with pillars is damaged during the coating process due to the delicate nanopillars being ripped off from the mold surface as the foils were fabricated at high P_{oil} of 22 bars. This could be avoided by running the process at lower nip pressure and optimizing the other process parameters such as T_C , V_R , and polymer feed rate, accordingly. This needs further investigation.

V. SUMMARY AND CONCLUSIONS

In this study, we have investigated replication of nanostructures in thermoplastic polymers, by a very high throughput, industrial process known as R2R-EC. Nanopits and nanopillars have been replicated with high replication

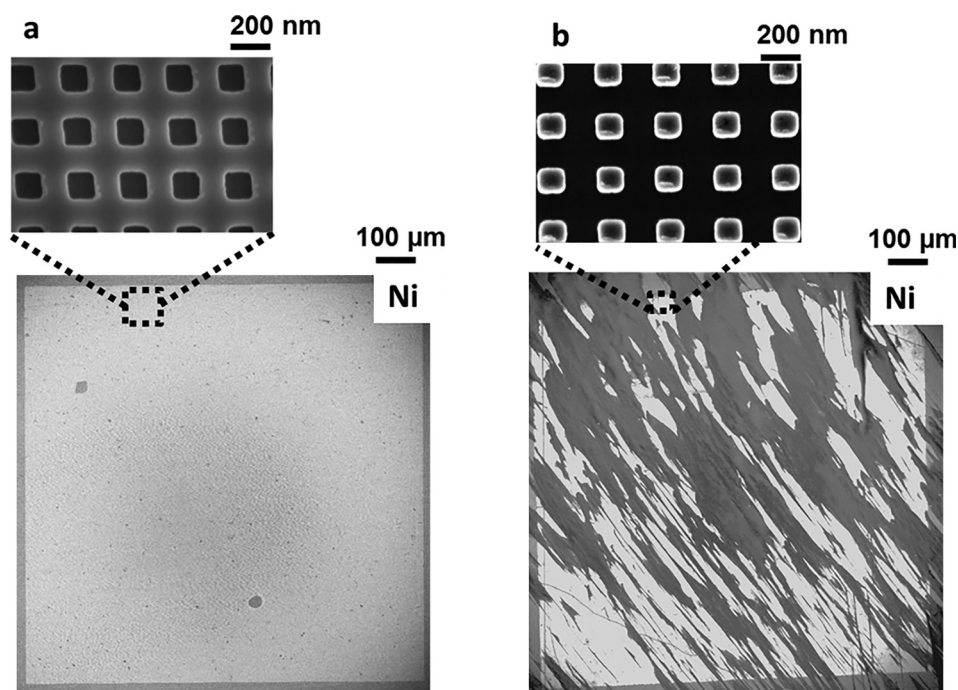


Fig. 8. (a) SEM images of Ni shim with nano-pits after R2R-EC; (b) SEM images of Ni shim with nano-pillars after R2R-EC.

fidelity, at high production rates ~ 5 m²/s. R2R-EC is a mature technology; it has the advantage of robust machinery, and availability of low cost and wide range of polymer materials. Thereby, we can manufacture large areas of functional nanostructured polymer foils at a very low cost. This could accelerate the integration of nanostructured materials in a broad range of consumer products, including optical, technical, functional surfaces and devices. It could also be used in cast molding of advanced materials where nanostructuring can result in enhanced properties, for example, photovoltaic, thermoelectric, electroactive, and electrostorage applications.

ACKNOWLEDGMENTS

This work was supported by the Danish Ministry of Higher Education and Science, through an industrial Ph.D. scholarship for Swathi Murthy (Grant No. 1355-00143). Nikolaj Mandsberg is acknowledged for help with COMSOL simulation. Colleagues at Inmold are acknowledged for their input and discussion.

¹K. Koch, B. Bhushan, Y. C. Jung, and W. Barthlott, *Soft Matter* **5**, 1386 (2009).

²A. B. Christiansen, J. Clausen, N. A. Mortensen, and A. Kristensen, *Appl. Phys. Lett.* **101**, 131902 (2012).

³K. Kumar, H. Duan, R. S. Hegde, S. C. W. Koh, J. N. Wei, and J. K. W. Yang, *Nat. Nanotechnol.* **7**, 557 (2012).

⁴K. Nagato, T. Hamaguchi, and M. Nakao, *J. Vac. Sci. Technol., B* **29**, 06FG10 (2011).

⁵P.-C. Chang and S.-J. Hwang, *J. Appl. Polym. Sci.* **102**, 3704 (2006).

⁶D. Yao and B. Kim, *Polym. Eng. Sci.* **42**, 2471 (2002).

⁷J. M. Stormonth-Darling, R. H. Pedersen, C. How, and N. Gadegaard, *J. Micromech. Microeng.* **24**, 075019 (2014).

⁸N. K. Andersen and R. J. Taboryski, *Microelectron. Eng.* **141**, 211 (2015).

⁹E. Søgaard, N. K. Andersen, K. Smistrup, S. T. Larsen, L. Sun, and R. J. Taboryski, *Langmuir* **30**, 12960 (2014).

¹⁰H. Schiff, C. David, M. Gabriel, J. Gobrecht, L. J. Heyderman, W. Kaiser, S. Köppel, and L. Scandella, *Microelectron. Eng.* **53**, 171 (2000).

¹¹C. Stuart and Y. Chen, *ACS Nano* **3**, 2062 (2009).

¹²H. Tan, A. Gilbertson, and S. Y. Chou, *J. Vac. Sci. Technol., B* **16**, 3926 (1998).

¹³S. H. Ahn and L. J. Guo, *Adv. Mater.* **20**, 2044 (2008).

¹⁴J. John, Y. Tang, J. P. Rothstein, J. J. Watkins, and K. R. Carter, *Nanotechnology* **24**, 505307 (2013).

¹⁵S. Kim, Y. Son, H. Park, B. Kim, and D. Yun, *Microsc. Microanal.* **21**, 164 (2015).

¹⁶C. Sollogoub, E. Felder, Y. Demay, J. F. Agassant, P. Deparis, and N. Mikler, *Polym. Eng. Sci.* **48**, 1634 (2008).

¹⁷S. Murthy *et al.*, *Adv. Eng. Mater.* **18**, 1 (2015).

¹⁸A. Telecka, S. Murthy, L. Schneider, H. Pranov, and R. Taboryski, *ACS Macro Lett.* **5**, 1034 (2016).

¹⁹Elders, Jansen, H. V. Jansen, M. Elwenspoek, and W. Ehrfeld, *IEEE Micro Electro Mech. Syst.* **1995**, 238.

²⁰S. Tanzi, P. F. Østergaard, and M. Matteucci, *J. Micromech. Microeng.* **22**, 115008 (2012).

²¹T. M. Yu, Y. M. Li, and B. Xu, *Gaofenzi Cailiao Kexue Yu Gongcheng* **25**, 153 (2009).

²²D. Yang, Z. Xu, C. Liu, and L. Wang, *Colloids Surf. A* **367**, 174 (2010).

²³D. Y. Kwok, L. K. Cheung, C. B. Park, and A. W. Neumann, *Polym. Eng. Sci.* **38**, 757 (1998).

²⁴B. Yang, X.-R. Fu, W. Yang, S.-P. Liang, N. Sun, S. Hu, and M.-B. Yang, *Macromol. Mater. Eng.* **294**, 336 (2009).

²⁵D. L. Dotson and P. Nygard, *Tappi 2008 Place Conference: Innovations in Flexible Consumer Packaging* (2008).

²⁶M. Tolinski, *Additives for Polyolefins: Getting the Most out of Polypropylene, Polyethylene and TPO* (Elsevier Science, Oxford, UK, 2015).

²⁷A. Peacock, *Handbook of Polyethylene: Structures: Properties: Applications* (Taylor & Francis, London, 2000).

²⁸J. T. Xu, P. J. Ding, Z. S. Fu, and Z. Q. Fan, *Polym. Int.* **53**, 1314 (2004).

²⁹J. E. K. Schawe, *J. Therm. Anal. Calorim.* **116**, 1165 (2014).

³⁰C. Vasile, *Handbook of Polyolefins* (Marcel Dekker, New York, 2000).